

Spatiotemporal mode-locked multimode fiber laser with dissipative four-wave mixing effect

Ming-Wei Qiu(邱明伟), Chao-Qun Cai(蔡超群), and Zu-Xing Zhang(张祖兴)†

Citation: Chin. Phys. B, 2022, 31 (**10**): 104207. DOI: 10.1088/1674-1056/ac6ee9
Journal homepage: http://cpb.iphy.ac.cn; http://iopscience.iop.org/cpb

What follows is a list of articles you may be interested in

Raman lasing and other nonlinear effects based on ultrahigh-*Q* CaF_2 optical resonator

Tong Xing(邢彤), Enbo Xing(邢恩博), Tao Jia(贾涛), Jianglong Li(李江龙), Jiamin Rong(戎佳敏), Yanru Zhou(周彦汝), Wenyao Liu(刘文耀), Jun Tang(唐军), and Jun Liu(刘俊)
Chin. Phys. B, 2022, 31 (**10**): 104204. DOI: 10.1088/1674-1056/ac8728

A 658-W VCSEL-pumped rod laser module with 52.6% optical efficiency

Xue-Peng Li(李雪鹏), Jing Yang(杨晶), Meng-Shuo Zhang(张梦硕), Tian-Li Yang(杨天利), Xiao-Jun Wang(王小军), and Qin-Jun Peng(彭钦军)
Chin. Phys. B, 2022, 31 (**8**): 084207. DOI: 10.1088/1674-1056/ac728f

Quality factor enhancement of plasmonic surface lattice resonance by using asymmetric periods

Yunjie Shi(石云杰), Lei Xiong(熊磊), Yuming Dong(董玉明), Degui Sun(孙德贵), and Guangyuan Li(李光元)
Chin. Phys. B, 2022, 31 (**1**): 014217. DOI: 10.1088/1674-1056/ac1332

Mode splitting and multiple-wavelength managements of surface plasmon polaritons in coupled cavities

Ping-Bo Fu(符平波) and Yue-Gang Chen(陈跃刚)
Chin. Phys. B, 2022, 31 (**1**): 014216. DOI: 10.1088/1674-1056/ac0e28

Brightening single-photon emitters by combining an ultrathin metallic antenna and a silicon quasi-BIC antenna

Shangtong Jia(贾尚曈), Zhi Li(李智), and Jianjun Chen(陈建军)
Chin. Phys. B, 2022, 31 (**1**): 014209. DOI: 10.1088/1674-1056/ac248c

---

SPECIAL TOPIC — Optical field manipulation

Spatiotemporal mode-locked multimode fiber laser with dissipative four-wave mixing effect

Ming-Wei Qiu(邱明伟), Chao-Qun Cai(蔡超群), and Zu-Xing Zhang(张祖兴)†

Advanced Photonic Technology Laboratory, College of Electronic and Optical Engineering & College of Microelectronics, Nanjing University of Posts and Telecommunications, Nanjing 210023, *China*

(Received 26 March 2022; revised manuscript received 3 May 2022; accepted manuscript online 12 May 2022)

The high degree of freedom and novel nonlinear phenomena of multimode fiber are attracting attention. In this work, we demonstrate a spatiotemporal mode-locked multimode fiber laser, which relies on microfiber knot resonance (MKR) via dissipative four-wave-mixing (DFMW) to achieve high-repetition-rate pulses. Apart from that, DFMW mode locking with switchable central wavelengths can also be obtained. It was further found that high pulse energy induced nonlinear effect of the dominant mode-locking mechanism transforming from DFMW to nonlinear Kerr beam cleaning effect (NL-KBC). The experimental results are valuable for further comprehending the dynamic characteristics of spatiotemporal mode-locked multimode fiber lasers, facilitating them much more accessible for applications.

Keywords: microfiber knot resonance (MKR), dissipative four-wave-mixing (DFMW), nonlinear Kerr beam cleaning effect (NL-KBC), multimode fiber laser

PACS: 42.60.Da, 42.60.Fc, 42.60.Jf, 42.65.Ky **DOI:** 10.1088/1674-1056/ac6ee9

1. Introduction

High-repetition-rate pulse fiber lasers can be widely used in optical communication to promote channel transmission rate of communication network,[1–3] materials processing,[4–6] nonlinear optical research,[7] and microwave photonics.[8] Especially ultrafast fiber laser[9–11] with high gain coefficient, wide wavelength range, good heat dissipation performance, and switchable laser mode, provides an ideal platform for high-repetition-rate pulse source research. So far, fiber lasers with high repetition-rate pulse generation have been realized by a variety of schemes, which can be divided into: harmonic mode-locking, based on fractional time domain effect and dissipative four-wave-mixing effect. In general, the pulse repetition rate of a passively mode-locked fiber laser is determined by the cavity mode spacing. Therefore, reducing cavity length is the most straightforward and simple method to obtain high-repetition-rate pulse. However, this obviously has a great limitation: the use of electronic device to achieve active mode-locking by control the parameters in the cavity is difficult to further improve the repetition frequency due to the bandwidth limitation inherent in electronic devices. Applications based on fractional time domain effect such as chirped Bragg grating[12–14] and long period fiber grating[15,16] require too much high initial frequency of optical signal and their structure and operation are complicated. The Fabry–Perot filter provided by Yoshida[17] was used to generate pulses with stable high repetition frequency, which was the first proposed scheme based on DFMW. Since then, high repetition-rate pulse based on DFMW has attracted much attention due to its simple structure and higher realizable frequency.

The key elements of dissipative four-wave mixing mode-locking technology are intracavity gain, multiwavelength filter and highly nonlinear components. Generally, the obtained pulse repetition frequency and laser wavelength are determined by the free spectral range (FSR) of the embedded comb filter and the central wavelength of the bandpass filter in the cavity. The widely used intra-cavity optical comb filtering includes Fabry–Perot filter, fiber grating, programmable optical processor, and microfiber knot resonator,[18–22] *etc*. Among all comb spectral filters, microfiber knot resonator device has become research hotspot due to its strong evanescent field effect, low insertion loss and perfect adaptation to all-fiber laser system. It is worth noting that most of high-repetition-rate pulse mode-locked fiber lasers at present are studied in single-mode fiber cavities. However, the high freedom degree of multimode fiber allows the generation of novel solitons and observation of more nonlinear phenomena. For example, a spatiotemporal mode-locked multimode fiber laser,[23] which relies on spatial beam self-cleaning via the nonlinear Kerr effect to attain high pulse energy with near Gaussian output beam shape was achieved. In addition to spatial beam cleaning[24–26] and spatial mode-locking,[27–29] instability of time and space, dispersive wave[30–32] have also been discovered. Therefore, the realization of high-repetition-rate pulse in multimode fiber laser is expected to observe various nonlinear optical phenomena.

In this paper, we demonstrate a wavelength-switchable spatiotemporal mode-locked multimode fiber laser, using MKR to realize dissipative four-wave-mixing (DFMW) mode-

†Corresponding author. E-mail: zxzhang@njupt.edu.cn

© 2022 Chinese Physical Society and IOP Publishing Ltd

locking. When the DFMW mode-locking operation starts automatically, pulses with high repetition rate of up to 69.21 GHz have been achieved, benefitting from the filtering characteristics of microfiber knot resonance and high nonlinearity implementation of highly nonlinear fiber (HNLF). Furthermore, the virtual few-mode fiber–multimode fiber filtering structure enables switchable wavelength DFMW mode-locking. In this regime, the laser-emitted switchable wavelength between $\sim$ 1035.3 nm and $\sim$ 1040.3 nm by changing the states of the polarization controllers. In addition, it was revealed that the nonlinear Kerr beam cleaning (NL-KBC) effect will result in normal dispersion soliton mode-locking in place of DFMW mode-locking when pulse energy reaches the NL-KBC threshold.

2. Device fabrication and characterization

A microfiber knot resonator is mainly composed of two parts: straight waveguide and curved waveguide, as schematically shown in Fig. 1. Due to the characteristics of evanescent field, power conversion mainly occurs in coupling region, therefore the light intensity in the coupling region is the largest after light transmission. MKR is manufactured by three main steps. Initially, fiber in the center should be tapered through the flame tapering method, then knotted and stretched continuously to shrink the ring diameter. Last, ensure that the desired MKR diameter and FSR are achieved and encapsulated with UV glue after tapering, to guarantee the firmness and easy access. The radius of tapered fiber of the used MKR is about 3 μm. As the fiber is stretched, the diameter of MKR becomes smaller. The performance of the MKR can be determined through observing the red light transmission of the micro-ring waveguide. When the light coupled to the micro-ring completely passes through the whole structure, the best filtering spectrum can be obtained.

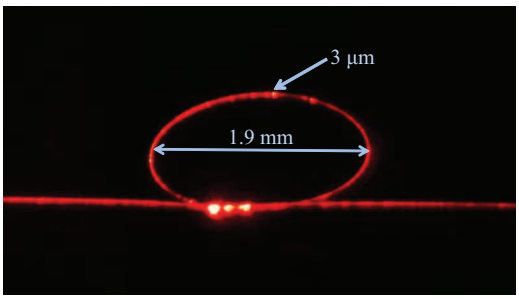


Fig. 1. Schematic structure of microfiber knot resonator under the microscope after light pass.

In order to ensure the excellent performance of the MKR and achieve the desired filtering effect, it is necessary to observe the transmission spectrum behind the light source and adjust the diameter of the MKR during the stretching process, as shown in Fig. 2(a). The broadband light source (BBS) is connected with the straight waveguide at one end, and another end is connected the optical spectrum analyzer (OSA) which is to measure the transmission spectrum of the MKR. Generally, when the diameter of the MKR is between 1 μm and 3 μm, the performance of the MKR filter is the best, its extinction is relatively large and interference spectrum is relatively flat. The transmission spectrum can also be affected by rotating the position of the micro-ring waveguide. Taking Fig. 2(b) for example, it shows transmission spectrum of the MKR used in this experiment, whose FSR is 0.12 nm. The diameter of the MKR is 1.9 mm. The extinction ratio of the filtering spectrum cannot be kept consistent which is mainly due to uneven heating of the tapered fiber caused by air fluctuation, but this does not affect the overall extinction ratio of the MKR and its filtering effect in the cavity. It should be noted that the fiber used in the MKR has a core diameter of 8.2 μm, a numerical aperture of 0.14, and a normalized frequency $V > 2.405$ at 1-μm wavelength band, which can support multiple modes of transmission.

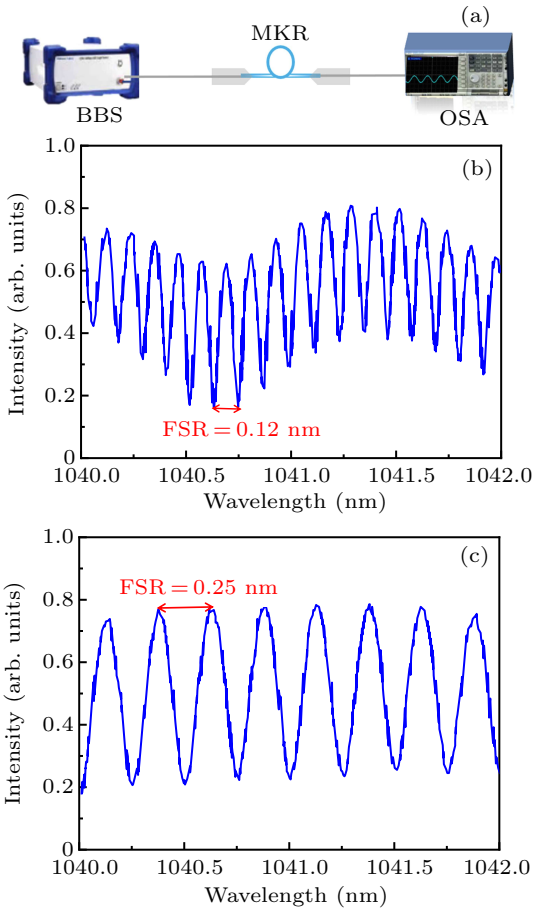


Fig. 2. (a) Experiment setups of spectrum measurement, (b) and (c) transmission spectrum of the fabricated MKRs.

3. Experiments and discussion

The experimental setup of the spatiotemporal mode-locked multimode fiber laser is depicted in Fig. 3. A 915-nm laser diode with maximum output power of 7 W is used as the pump source, launched into an ytterbium-doped multimode

fiber (Yb MMF) through a 915-nm/1064-nm beam combiner. It contains a 2.2-m graded-index multimode fiber (GIMF) with 50-μm core diameter, a double-cladding multimode gain fiber of 4.5 m. The gain fiber supports about 3 spatial modes, and GIMF can support dozens of spatial modes. Due to the different core diameters of the fibers, most transverse modes are eliminated, which serves as a virtual spatial filter. There is a bulky polarizing beam splitter (PBS) and a free space isolator in free space part of the laser cavity, which is coupled with fiber part by two lenses (L1 and L2). With the PBS and two polarization controllers (PCs), nonlinear polarization evolution (NPE) is implemented as an artificial absorber. The two PCs are placed before and after the space structure. MKR acts as a comb filter in the cavity. A 200-m long highly nonlinear fiber provides high nonlinearity into the cavity to promote the occurrence of four-wave mixing, so that the gain modes transfer energy to the higher-order mode. Four-wave mixing causes all modes to be in constant phase relation as the process repeats itself, resulting in an impulse train whose repetition rate is determined by the free spectral range of MKR.

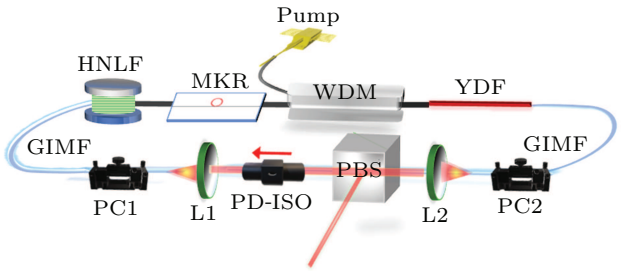


Fig. 3. Schematic diagram of the spatiotemporal mode-locked multimode fiber laser. Yb MMF: double cladding Yb-doped multimode fiber; GIMF: graded-index multimode fiber; PC: polarization controller; L1, L2: lens; PD-ISO: polarization-dependent isolator; PBS: polarization beam splitter; MKR: microfiber knot resonator; HNLF: highly nonlinear fiber.

In this experiment, with the increase of pump power and adjustment of polarization controller, spatiotemporal mode-locking operation can be achieved due to the DFMW. We performed a detailed characterization of the laser when the pump power is set to 4.2 W. Owing to the instantaneous pump power and high nonlinearity introduced by the HNLF, laser shifts to the regime of DFMW mode-locking where optical frequency comb spectra emerges. As expected, a typical output of DFMW spatiotemporal mode-locking operation with a high-repetition-rate pulse was measured, as shown in Fig. 4. Its output spectrum is shown in Fig. 4(a). The central wavelength locates at 1040.3 nm. According to the output spectrum, the FSR of 0.12 nm corresponds to the MKR diameter of 1.9 mm. The theoretical calculation shows that the pulse repetition frequency is 33.22 GHz. As also noted, the output beam profile is a high multi-mode beam profile due to the low pulse energy in the cavity. In order to verify the realization of DFMW, we detected the output pulse, as shown in Fig. 4(b). It shows the time interval of the output pulse string is 30.1 ps and its corresponding repetition frequency is 33.22 GHz, consistent with the theoretical calculation value.

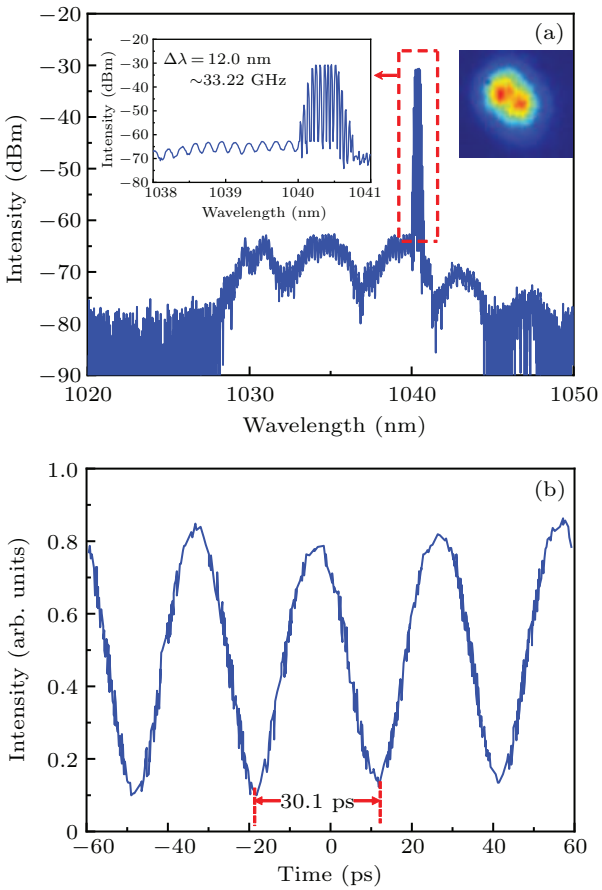


Fig. 4. The generation of 33.22-GHz high-repetition-rate pulses: (a) mode-locked spectrum, (b) pulse train.

Meanwhile, we can see that the output spectrum has a larger filter envelope with a spacing of about 5 nm contrasted with the MKR filter, which is obviously due to the virtual few-mode fiber-MMF (FM-MMF) filtering structure. This structure is mainly constituted by the 10-μm/125-μm fiber (YDF) and the GIMF. By carefully adjusting the PCs, DFMW spatiotemporal mode-locking operation with different central wavelengths can be obtained, as shown in Fig. 5. Similarly, we have tried to further reduce the diameter of the MKR to change the free spectral range of filtering, and achieved DFMW mode-locking with higher repetition rate. These results demonstrate the versatility of MKR during high-repetition-rate pulse generation in multimode fiber lasers.

In a spatiotemporal mode-locked MMF cavity, the nonlinear energy exchange between transverse modes can be caused by nonlinear gain, nonlinear loss, and pulse energy in cavity. It is shown in the recent exploration of spatiotemporal mode-locked multimode fiber lasers that the NL-KBC effect induced by GIMF can improve beam quality and enhance average power in MMF cavity. The NL-KBC effect refers to the fact that energy of the high-order mode will be irreverently coupled to the fundamental mode, which makes the

high-intensity pulsed multimode beam profile transform into a nearly Gaussian beam. It is worth noting the pulse energy needs to reach the required threshold, and pump power required for NL-KBC is distinct with different wavelength spatiotemporal mode-locked multimode lasers.[33] Based on this, an interesting phenomenon occurred when power exceeds 6.2 W. Instead of quasi-DFMW spectrum, a broadband and beam autoselection mode-locked spectrum can be observed, as shown in Fig. 6(a). Compared to the DFMW mode-locking spectrum, it is broader and has the similar steep edges as the dissipative solitons in the all-normal-dispersion laser. It can be found that the spectrum still has the characteristics of MKR filtering and the spectral interval of fine structure conforms to the FSR of the MKR. The difference is the pulse repetition rate plummets and the interval of output pulses is 925.9 ns, as shown in Fig. 6(b), and the corresponding pulse energy measured is 13.4 nJ. Figure 6(c) plots corresponding detailed radio frequency (RF) spectrum around fundamental pulse repetition rate, which peaks at 1.08 MHz with signal-to-noise ratio (SNR) of 42 dB. The beam profile shows beam energy distribution on the profile map, related to the transverse modes distribution, as shown in interior illustration of Fig. 6(a). It has no longer a high-order-mode beam, but a Gaussian center and a background composed of several high-order modes. And with the increase of pulse energy, the purity of the output beam can be further improved, up to 86% in our cavity. In order to show the NL-KBC effect happened in the cavity directly, we compared output beam profiles under different pump powers, shown in Fig. 6(d). This clearly shows the obvious transformation of the beam profile when the NL-KBC effect occurs. That means competition between nonlinear effects also exists in multimode cavity. When pulse energy reaches the NL-KBC threshold, it will instead of four-wave mixing to play a dominant role in the nonlinear effect in the cavity.

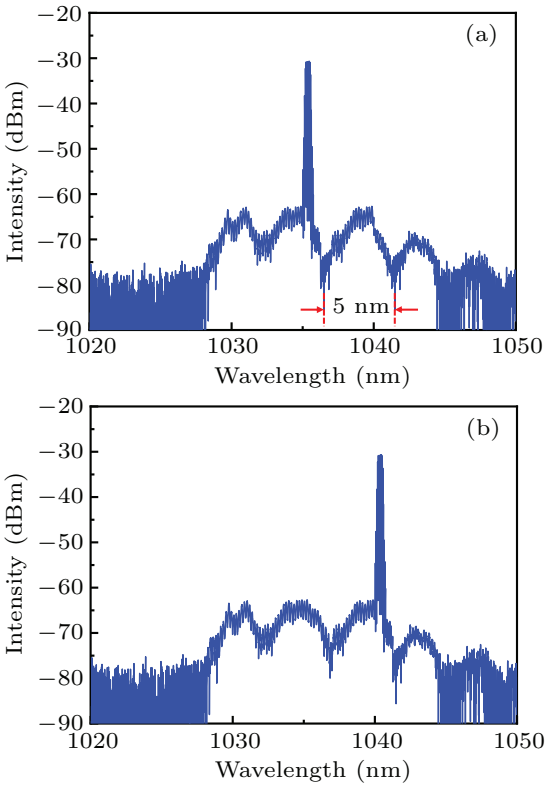


Fig. 5. Wavelength switchable operation from (a) 1035.3 nm to (b) 1040.3 nm.

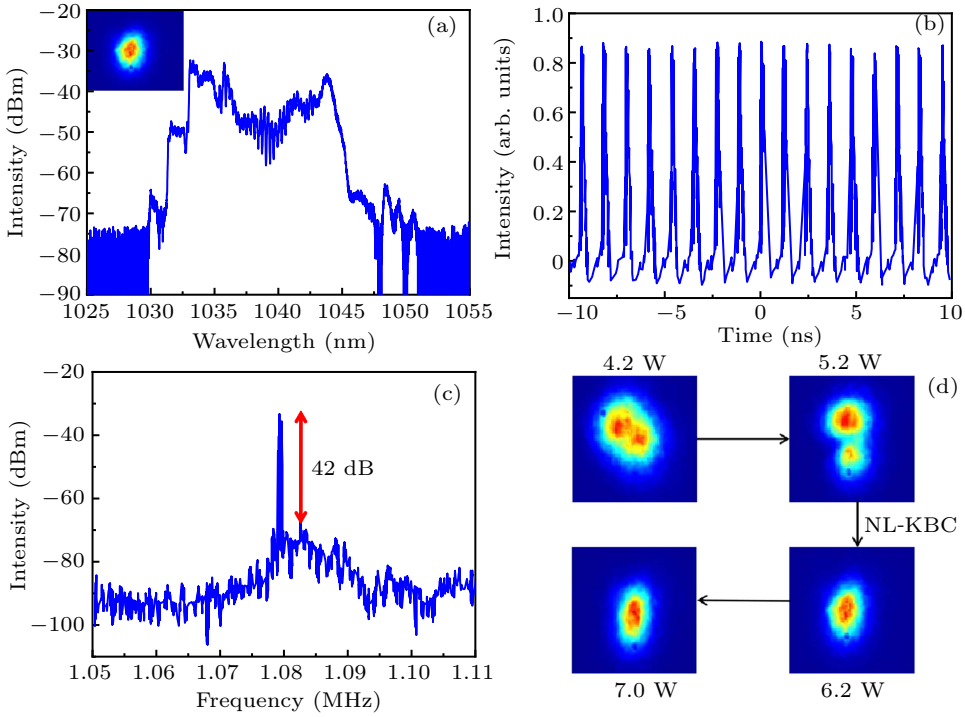


Fig. 6. Dissipative soliton mode-locking with higher pump power: (a) optical spectrum (inset: the corresponding beam profiles), (b) pulse train, (c) RF spectrum with a resolution bandwidth of 1 Hz, (d) beam profile both under different pump powers.

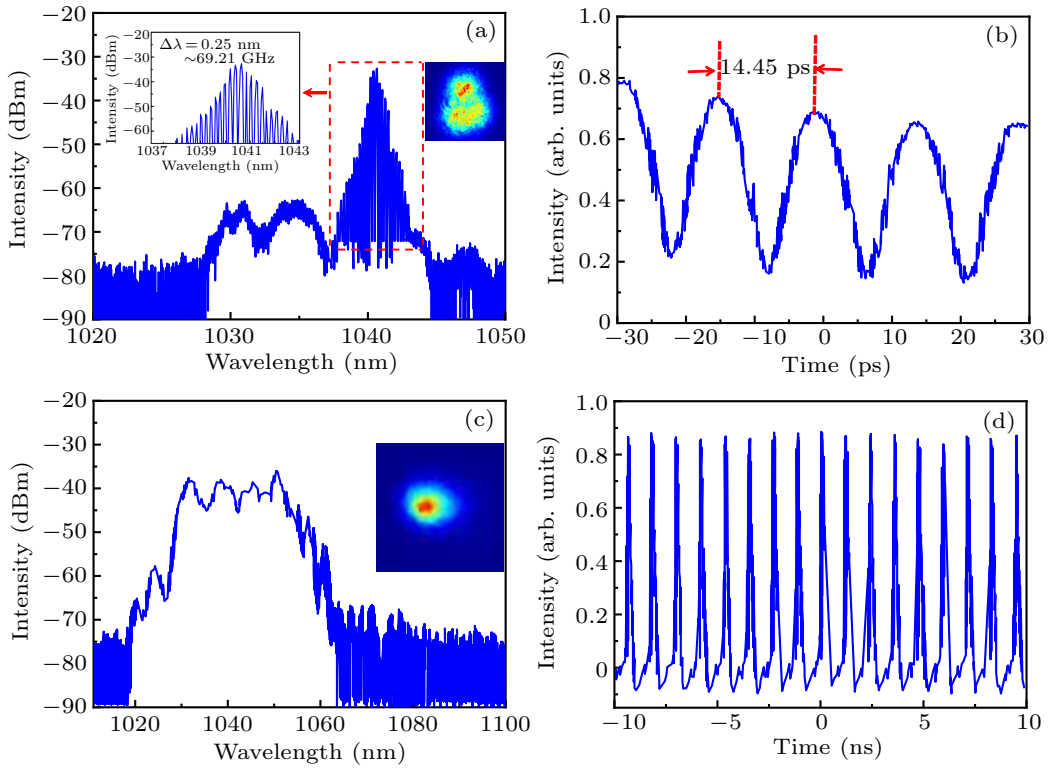


Fig. 7. The output characteristics with 0.25-nm FSR of the used MKR: DFMW mode-locking spectrum, (b) corresponding pulse train, (c) dissipative soliton mode-locking spectrum, (d) pulse train.

All the experimental results shown so far are based on the MKR with an FSR of 0.12 nm. In the discussion of MKR in the previous section, we mentioned that the advantages of microfiber knot compared with other filters are mainly reflected in the adjustable FSR. Therefore, we further reduced the diameter of MKR and applied it to the same multimode fiber laser. When the pump power was set to 4.5 W and the polarization controller was fine-tuned, the DFWM mode-locking spectrum as shown in Fig. 7(a) can be acquired. The diameter of MKR at this case turns into 1.4 mm and its FSR is 0.25 nm. The mode-locking center wavelength is located at 1040 nm and the comb spectrum interval is 0.25 nm which meets the ideal expectation, and the measured time interval of the output pulse train is 14.45 ps, as shown in Fig. 7(b), the relevant repetition rate is 68.9 GHz, confirming that DFWM mode-locking has been realized. Note that the output beam profile is in a high multimode state, similar to the experiment result with 0.12-nm MKR. Meanwhile, we increased the pump power, making higher pulse energy. After fine-tuning PC, with the pump power of 6 W, the dissipative soliton mode-locking spectrum which is different from the DFWM mode-locking spectra was also observed [shown in Fig. 7(c)], and the output beam profile was similarly turned into a nearly Gaussian beam profile, indicating that the nonlinear Kerr beam self-cleaning effect occurs. Similar experiment results using different MKRs verify the competitive relationship between different nonlinear effects in multimode fiber laser. When the pulse energy in the cavity is low, four-wave mixing effect dominates and the DFWM mode-locking is achieved attributed to the use of MKR, getting high-repetition-rate pulse and comb spectrum. When pulse energy reaches the threshold of NL-KBC, the introduction of irreversible NL-KBC effect by GIMF will couple the higher-order mode energy into the lower-order mode, inhibiting production of four-wave mixing effect and occupying the dominant position. And the traditional mode-locked spectrum with normal dispersion can be observed. The output pulse repetition frequency is no longer determined by the FSR of the MKR, but mainly by the length of the cavity.

4. Conclusions

In conclusion, we have reported a spatiotemporal mode-locked multimode fiber laser with MKR. High-repetition-rate pulse output has been realized by DFMW in highly nonlinear fiber. Wavelength-switchable DFMW operation can be further achieved on account of a virtual FM-MMF filter structure. It was also found that the pulse energy in the cavity determines the dominant role of nonlinear effects for mode-locking. When the pulse energy in the cavity is high enough, the NL-KBC effect can transform the beam profile from high-order mode to Gaussian profile irreversibly. We believe that the discovery of this phenomenon will not only provide a new idea for the application of MKR to generate high-repetition-rate pulse train in multimode fiber lasers, but provide a research platform for the observation of more nonlinear phenomena in multimode fiber lasers.

Acknowledgements

Project partially supported by the National Natural Science Foundation of China (Grant Nos. 91950105 and 62175116) and the 1311 Talent Plan of Nanjing University of Posts and Telecommunications.

References

[1] Essiambre R, Kramer G, Winzer P, Foschini G and Goebel B 2010 *J. Lightwave Technol.* **28** 662
[2] Yam S H and Achten F 2007 *J. Opt. Netw.* **6** 527
[3] Torres C V, Schroder J, Fulop A L, Mazur M, Lundberg L, Helgason O, Karlsson M and Andreksonet P 2019 *J. Lightwave Technol.* **37** 1663
[4] Harun S W, Saidin N, Zen D I M, Ali N M, Ahmad H, Ahmad F and Dimyati K 2013 *Chin. Phys. Lett.* **30** 094204
[5] Nava G, Osellame R, Ramponi R and Vishnubhatla K C 2013 *Opt. Mater. Express* **3** 612
[6] Huang Y, Xie X, Li M, Xu M and Long J 2021 *Opt. Express* **29** 4453
[7] Harshavardhan Reddy P, Kadir N A A, Paul M C, Das S, Dhar A, Ismail E I, Latiff A A and Harun S W 2017 *Chin. Phys. Lett.* **34** 084203
[8] Gu C, Zuo Z, Luo D, Peng D, Di Y, Zou X, Yang L and Li W 2019 *Opt. Lett.* **44** 5848
[9] Cheng H, Wang W, Zhou Y, Qiao T, Lin W, Guo Y, Xu S and Yang Z 2018 *Opt. Express* **26** 16411
[10] Zhao Q, Gao G, Cong Z, Zhang Z, Liu G, Liu Z, Zhang X and Zhao Z 2022 *Opt. Express* **30** 3611
[11] Zhao Z, Jin L, Set S Y and Yamashita S 2021 *Opt. Lett.* **46** 3621
[12] Sakamoto T and Yoshioka K 2021 *Opt. Lett.* **46** 4642
[13] Magne J, Bolger J, Rochette M, LaRochelle S, Chen L R, Eggleton B J and Azana J 2006 *J. Lightwave Technol.* **24** 2091
[14] Hong K H, Siddiqui A, Moses J, Gopinath J, Hybl J, Ilday F O, Fan T Y and Kartner F X 2008 *Opt. Lett.* **33** 2473
[15] Regan B J, Nikogosyan D N, Paipulas D, Kudriaov V and Sirutkaitis V 2012 *Opt. Fiber Technol.* **18** 88
[16] Krcmarík D, Slavík R, Park Y and Azana J 2009 *Opt. Express* **17** 7074
[17] Yoshida E and Nakazawa M 1997 *Opt. Lett.* **22** 1409
[18] Jasim A A, Zulkifli A Z, Muhammad M Z, Ahmad H and Harun S W 2012 *Chin. Phys. Lett.* **29** 084204
[19] Guan H, Li Z Y, Shen H H, Wang R and Yu Y D 2017 *Chin. Phys. Lett.* **34** 084204
[20] Peccianti M, Pasquazi A, Park Y, Little B E, Chu S T, Moss D J and Morandotti R 2012 *Nat. Commun.* **3** 85
[21] Ding Z X, Huang Z N, Chen Y, Mou C B, Lu Y Q and Xu F 2020 *Adv. Photon.* **2** 026002
[22] Liu M, Tang R, Luo A P, Xu W and Luo Z C 2018 *Photon. Res.* **6** C1
[23] Tegin U, Rahmani B, Kakkava E, Psaltis D and Moser C 2020 *Adv. Photon.* **2** 056005
[24] Niang A, Levchenko A, Semjonov S, Lipatov D and Egorova O 2020 *Photon. J.* **12** 1
[25] Tegin U and Ortaç B 2017 *Photon. Technol. Lett.* **24** 1
[26] Hansson T, Tonello A, Mansuryan T, Mangini F, Zitelli M, Ferraro M, Niang A, Crescenzi R, Wabnitz S and Couderc V 2020 *Opt. Express* **28** 24005
[27] Qin H, Xiao X, Wang P and Yang C 2018 *Opt. Lett.* **43** 1982
[28] Tegin U, Kakkava E, Rahmani B, Psaltis D and Moser C 2019 *Optica* **6** 1412
[29] Ma Z L, Long J G, Lin W, Hong W, Cui H, Luo Z, Xu W, Likhachev M, Aleshkina S, Mashinsky V, Yashkov M and Luo A 2021 *Opt. Express* **29** 9465
[30] Wright L G, Wabnitz S, Christodoulides D and Wise F W 2015 *J. Lightwave Technol.* **115** 223902
[31] Coen S and Haelterman M 2001 *Opt. Lett.* **26** 39
[32] Chen G, Li W, Wang G, Zhang W, Zeng C and Zhao W 2019 *Photon. Res.* **7** 187
[33] Qiu M W, Chen M M and Zhang Z X 2021 *Photon. Technol. Lett.* **33** 1073